

Scalar Perturbations on Lemaître-Tolman-Bondi Spacetimes

J. P. Zibin*

Department of Physics & Astronomy, University of British Columbia, Vancouver, BC, V6T 1Z1 Canada

(Dated: November 3, 2018)

In recent years there has been growing interest in verifying the horizon-scale homogeneity of the Universe that follows from applying the Copernican Principle to the observed isotropy. This program has been stimulated by the discovery that a very large void, centred near us, can explain supernova luminosity distance measurements without dark energy. It is crucial to confront such models with as wide a variety of data as possible. With this application in mind, I develop the relativistic theory of linear scalar perturbations on spherically symmetric dust (Lemaître-Tolman-Bondi) spacetimes, using the covariant $1+1+2$ formalism. I show that the evolution of perturbations is determined by a small set of new linear transfer functions. If decaying modes are ignored (to be consistent with the standard inflationary paradigm), the standard techniques of perturbation theory on homogeneous backgrounds, such as harmonic expansion, can be applied, and results closely paralleling those of familiar cosmological perturbation theory can be obtained.

PACS numbers: 98.80.Cq, 98.80.Jk

I. INTRODUCTION

Since shortly after the discovery of the cosmic microwave background (CMB) radiation, it has been clear that the Universe is very nearly isotropic, with departures from uniformity in the CMB temperature at the level of 1 part in 10^5 (apart from the dipole of presumably kinetic origin). Since the CMB comes to us from the greatest visible distances, that observed isotropy tells us about the symmetry of spacetime on the largest observable scales. The natural assumption is that this isotropy cannot be an accident of our location, and that *any* observer would see essentially the same picture, regardless of where they were located. This notion is known as the Copernican Principle, and implies that the Universe is essentially homogeneous on the largest observable scales.

However, cosmologists are in the business of determining the nature of the Universe through observation and deduction, rather than through philosophical postulate. As unappealing as it may appear, a Universe with substantial radial inhomogeneity on the largest scales is consistent with the observed isotropy. Galaxy surveys are a means to quantify homogeneity, but are limited in their reach (see, e.g., [1, 2]), and *radial* inhomogeneity is difficult to disentangle from redshift-dependent effects such as evolution. Direct observational constraints on homogeneity over distances comparable to that to the last scattering surface, which emitted the CMB, are unavailable.

A few novel proposals exist in the literature for observational signatures of radial inhomogeneity. The CMB radiation we observe is partly scattered from within our past light cone, and this may allow us to constrain inhomogeneity [3, 4]. A consistency relation between luminosity distances and the Hubble rate, which must be satisfied for homogeneous and isotropic Friedmann-

Robertson-Walker (FRW) models, has been discussed [5]. Recently the time drift of cosmological redshifts was proposed as a test of homogeneity [6].

This might appear as something of a “dotting the i’s and crossing the t’s” cosmological exercise, if not for the realization nearly ten years ago that a particular form of radial inhomogeneity can actually mimic the effect of accelerated expansion in supernova data [7]. The model studied was the spherically symmetric dust, or Lemaître-Tolman-Bondi (LTB) spacetime [8, 9, 10]. Since that time many studies have confirmed and elaborated upon this idea (see, e.g., [11, 12, 13, 14]; more references can be found in the brief review [15]). The basic idea is quite simple: the increasing expansion rate *in time* that standard dark energy models describe is replaced with increasing expansion rate *towards the centre* of a radial inhomogeneity. These two possibilities are difficult to distinguish if our observations are limited to the surface of our past light cone.

To get the sign of the effect right (apparent acceleration rather than deceleration), we must be near the centre of an *underdensity*, or void. The void must be *nonlinear* today if it is to mimic the zeroth-order effect of acceleration. Additionally, the void must extend to a great distance, namely several hundred Mpc, corresponding to the redshifts at which the relevant supernova data lies, $z \simeq 0.2 - 1$. The presence of such a large void is strongly at odds with the standard picture of structure formation, where the largest nonlinear voids today appear at scales of tens of Mpc. Nevertheless, the difficulties with understanding the theoretical basis for dark energy, as well as the coincidence problem, have led many researchers to examine such void models as alternatives to dark energy.

In the context of void models for acceleration, and, more generally, considering the more fundamental issue of large-scale homogeneity, it is very important to constrain radial homogeneity using actual observations. Clearly, the more data we use to do this the better. LTB models contain one (technically two; see below) free ra-

*Electronic address: zibin@phas.ubc.ca

dial functions which could be adjusted to optimize the fit to any single data set. Therefore it is with complementary data that our greatest hope lies in constraining such models. Surprisingly, few studies of void models for acceleration have gone beyond fitting to supernova data. Notable exceptions are Refs. [11, 13], who considered CMB data, and, very recently, Ref. [14], who considered a wider range of data including CMB and baryon acoustic oscillations.

One important class of data which has remained out of reach so far involves the behaviour of scalar density perturbations, i.e. the structure we observe on all scales. The evolution of this structure at *linear* order is necessarily affected by the presence of a large radial inhomogeneity or void in the *zeroth*-order background. While luminosity and angular diameter distances and redshifts are simple to calculate in LTB spacetimes, no one has yet studied perturbed LTB spacetimes. It may indeed appear daunting to tackle perturbations on a background spacetime which is not itself homogeneous [40]. However, with the appropriate tools, the task turns out to be not too much more difficult than the familiar perturbation theory on FRW backgrounds.

Here I develop a formalism to study the evolution of linear scalar perturbations on LTB backgrounds. The approach is fully general relativistic, employing the covariant $1+1+2$ formalism (see, e.g., [16, 17, 18]), which generalizes the standard $1+3$ approach (see [19] for a recent review). This approach, while less familiar than the metric-based approach to many, offers several advantages, both in providing concise dynamical expressions which manifestly respect the symmetries of the problem, as well as in emphasizing physical and in principle observable quantities.

I do not develop the theory of perturbations on LTB backgrounds in complete generality. Rather, I target the development towards application to realistic void profiles that are able to mimic acceleration. My only approximation is to ignore the coupling between scalar and tensor modes that curved backgrounds generally facilitate. I argue that for the applications of interest, the sourced tensors will have a negligible effect on the scalar dynamics. I determine only the 2-scalar degrees of freedom, but these should be the most relevant observationally. While the background is taken to be spherically symmetric, the perturbations are completely free (apart from the linear and scalar approximations).

It is important to choose void profiles that can fit within the standard inflationary paradigm, according to which at early times the Universe is expected to be very homogeneous. [One possible origin for a large void (and perhaps the most conservative) is as a rare, large amplitude fluctuation within the primordial Gaussian random field produced during inflation. The only other origin discussed for such a void appears to rely on highly speculative quantum cosmological ideas [20]]. Therefore, such a void cannot contain a significant *decaying* mode today, without spoiling primordial homogeneity. It is dif-

ficult enough to believe that such a large void exists and is centred near us, without compounding the difficulties by giving up the standard inflationary scenario as well! Dropping the decaying mode also reduces our freedom to tweak an LTB model to fit data, so this should yield more predictive models.

The dropping of the decaying mode provides a tremendous advantage in treating perturbations. Namely, since at early times the spacetime approaches FRW with linear fluctuations (one of which is the large proto-void itself), all of the familiar tools used in perturbation theory on FRW can be applied at those early times, such as harmonic expansion and the use of statistical relations satisfied by primordial Gaussian random fields. At late times, when the LTB background has become nonlinear, it will be possible to relate the scalar fluctuations to the initial conditions using a small set of new LTB linear transfer functions. It should be possible to address many of the important observational signatures of structure using this formalism. The current work lays out the formalism; applications to specific observations will follow [21].

I begin in Sec. II with a brief review of the relevant covariant $1+3$ formalism. Next I describe the application of the further $1+1+2$ decomposition to LTB models, before describing the exact LTB solution. Section III lays out the perturbation formalism, beginning with a careful definition of perturbations, before introducing the LTB transfer functions, and then setting up the initial conditions. Finally, Sec. IV presents some numerical results. I use signature $(-, +, +, +)$ and set $c = 1$ throughout.

II. $1+1+2$ DECOMPOSITION FOR LTB BACKGROUND

In the $1+3$ covariant approach to relativistic cosmology (see, e.g., [19] for a recent review), all quantities are decomposed with respect to a fundamental congruence of timelike worldlines, with tangent vector field u^μ . A spacetime containing a single type of matter (pressureless dust in the case of LTB) is perfectly suited to a covariant treatment using the $1+3$ decomposition, since the comoving worldlines naturally define a special timelike congruence, at least until worldlines intersect. When the congruence is twist-free, it is hypersurface-orthogonal [22], and hence we can define spacelike *slices* everywhere orthogonal to the congruence.

The spherical symmetry of the LTB background is well suited to further decomposing matter and metric quantities according to a $1+1+2$ decomposition, since a spacelike congruence on each slice is naturally provided by the radial direction. In this section I provide a covariant $1+1+2$ treatment of the LTB background, along the lines of that presented in Refs. [17, 18, 23]. This will set the stage for the treatment of linear perturbations in Sec. III.

A. 1 + 3 decomposition

To begin, we will need a set of quantities which completely describe the spacetime in terms of the 1 + 3 decomposition. Henceforth u^μ will always be taken to be the timelike vector field tangent to the comoving worldlines, with normalization $u^\mu u_\mu = -1$. The tensor

$$h^\mu{}_\nu \equiv \delta^\mu{}_\nu + u^\mu u_\nu \quad (1)$$

projects orthogonal to u^μ . When the twist vanishes, we can consider $h_{\mu\nu}$ to be the metric tensor for the orthogonal spacelike slices, and we can also use $h_{\mu\nu}$ to define a spatially projected covariant derivative according to

$$D_\mu T_{\nu_1 \nu_2 \dots \nu_n} \equiv h^\lambda{}_\mu h^{\sigma_1}{}_{\nu_1} h^{\sigma_2}{}_{\nu_2} \dots h^{\sigma_n}{}_{\nu_n} T_{\sigma_1 \sigma_2 \dots \sigma_n; \lambda}, \quad (2)$$

for any tensor $T_{\nu_1 \nu_2 \dots \nu_n}$ orthogonal to u^μ in all of its indices. To describe the time evolution of any covariant quantity, we employ the proper time derivative along the comoving worldlines,

$$\dot{T}_{\mu\nu\dots\rho} \equiv u^\kappa T_{\mu\nu\dots\rho; \kappa} \quad (3)$$

for any tensor quantity $T_{\mu\nu\dots\rho}$. Finally, angled brackets around tensor indices indicate the spatially projected, symmetric, and trace-free part:

$$T^{(\mu\nu)} \equiv \left(h^{\mu}{}_\kappa h^{\nu}{}_\lambda - \frac{1}{3} h^{\mu\nu} h_{\kappa\lambda} \right) T^{\kappa\lambda}, \quad (4)$$

and the tensorial curl is defined by

$$\text{curl} T_{\mu\nu} \equiv \epsilon_{\kappa\lambda(\mu} D^\kappa T_{\nu)}{}^\lambda. \quad (5)$$

Here $\epsilon_{\mu\nu\lambda} \equiv \epsilon_{\mu\nu\lambda\kappa} u^\kappa$, where $\epsilon_{\mu\nu\lambda\kappa}$ is the totally antisymmetric four-volume element.

We can characterize the comoving congruence kinematically via the following standard decomposition of the covariant derivative $u_{\mu; \nu}$:

$$u_{\mu; \nu} = \frac{1}{3} \theta h_{\mu\nu} + \sigma_{\mu\nu} + \omega_{\mu\nu} - a_\mu u_\nu. \quad (6)$$

The scalar θ measures the local volume rate of expansion of the congruence, while trace-free, symmetric tensor $\sigma_{\mu\nu}$ and antisymmetric $\omega_{\mu\nu}$ measure the local rates of shear and twist of the congruence, respectively. The vector $a_\mu \equiv u_{\mu; \rho} u^\rho$ measures the acceleration of the comoving worldlines. Each of $\sigma_{\mu\nu}$, $\omega_{\mu\nu}$, and a_μ are orthogonal to u^μ in all of their indices.

We will also need two tensors derived from the Weyl tensor, $C_{\mu\nu\lambda\rho}$, which characterizes the nonlocal part of the gravitational field. The electric, $E_{\mu\nu}$, and magnetic, $H_{\mu\nu}$, parts of the Weyl tensor are defined by

$$E_{\mu\nu} \equiv C_{\mu\lambda\nu\rho} u^\lambda u^\rho, \quad H_{\mu\nu} \equiv \frac{1}{2} \epsilon_\mu{}^{\lambda\rho} C_{\lambda\rho\nu\kappa} u^\kappa. \quad (7)$$

The electric Weyl tensor describes the nonlocal tidal gravitational field, while the magnetic part describes, at least at linear order, propagating gravitational waves. Both $E_{\mu\nu}$ and $H_{\mu\nu}$ are fully orthogonal to u^μ . For the case of a homogeneous and isotropic FRW cosmology, we have $\theta = 3H$, where H is the Hubble rate, and $\sigma_{\mu\nu} = \omega_{\mu\nu} = a_\mu = E_{\mu\nu} = H_{\mu\nu} = 0$.

If the pressure (and hence the anisotropic stress) vanishes, then the matter content is described by the simple stress-energy tensor

$$T^{\mu\nu} = \rho u^\mu u^\nu, \quad (8)$$

with ρ the local energy density as judged by comoving observers. The spatially projected stress-energy conservation law, $h^\kappa{}_\nu T^{\mu\nu}{}_{; \mu} = 0$, i.e. the momentum conservation law, becomes

$$a^\mu = 0 \quad (9)$$

(as long as $\rho \neq 0$), representing the familiar result that comoving dust worldlines are geodesic.

The above kinematical, gravitational, and matter degrees of freedom provide a complete description of the spacetime. It only remains to specify their evolution. The twist $\omega_{\mu\nu}$ of the congruence is a special case, and satisfies the evolution equation [19]

$$h^\mu{}_\nu \dot{\omega}^\nu = -\frac{2}{3} \theta \omega^\mu + \sigma^\mu{}_\nu \omega^\nu, \quad (10)$$

where $\omega_\mu \equiv \epsilon_{\mu\nu\lambda} \omega^{\nu\lambda} / 2$. Therefore, if the twist vanishes initially, it vanishes for all time. Henceforth the twist will always be set to zero. This amounts to ignoring the presence of vector perturbation modes at linear order, which is a reasonable assumption within the standard inflationary scenario. Also, this means we can define spacelike slices orthogonal to the comoving flow.

The evolution of the remaining quantities is determined by the following set of equations [19]:

$$\text{Energy conservation:} \quad \dot{\rho} = -\theta\rho \quad (11)$$

$$\text{Raychaudhuri:} \quad \dot{\theta} = -\frac{\theta^2}{3} - 4\pi G\rho - \sigma^{\mu\nu}\sigma_{\mu\nu} \quad (12)$$

$$\text{Shear evolution:} \quad \dot{\sigma}_{\langle\mu\nu\rangle} = -\frac{2}{3}\theta\sigma_{\mu\nu} - \sigma_{\lambda\langle\mu}\sigma^{\lambda}_{\nu\rangle} - E_{\mu\nu} \quad (13)$$

$$E_{\mu\nu} \text{ evolution:} \quad \dot{E}_{\langle\mu\nu\rangle} = -\theta E_{\mu\nu} + 3\sigma_{\lambda\langle\mu}E^{\lambda}_{\nu\rangle} - 4\pi G\rho\sigma_{\mu\nu} + \text{curl}H_{\mu\nu} \quad (14)$$

$$H_{\mu\nu} \text{ evolution:} \quad \dot{H}_{\langle\mu\nu\rangle} = -\theta H_{\mu\nu} + 3\sigma_{\lambda\langle\mu}H^{\lambda}_{\nu\rangle} - \text{curl}E_{\mu\nu}. \quad (15)$$

The evolution of each quantity is determined by a damping term, proportional to the expansion (possibly corrected by the shear), together with coupling terms, such as the direct coupling between shear and the tidal field $E_{\mu\nu}$, and the coupling between electric and magnetic Weyl curvature via the curl terms, which supports the propagation of gravitational waves. This set of equations would have been significantly more complicated had we not chosen u^μ to be comoving, with extra terms involving the momentum density and acceleration a^μ . In addition, the initial conditions must satisfy a set of initial-value constraint equations, although we will not need the explicit form of the constraints here.

B. 1 + 1 + 2 decomposition

Under spherical symmetry, each comoving-orthogonal slice contains a preferred spacelike congruence with radial tangent vector r^μ , where $r^\mu r_\mu = 1$. By analogy with the tensor h^μ_ν defined in Eq. (1), which projects into the slices, we can define a tensor $s_{\mu\nu}$ by

$$s_{\mu\nu} \equiv h_{\mu\nu} - r_\mu r_\nu, \quad (16)$$

which projects orthogonally to both u^μ and r^μ . A 2-surface lying in a slice and orthogonal to r^μ will be called a *sheet*. (The sheets are ordinary 2-spheres under spherical symmetry.)

Any symmetric, trace-free tensor $T_{\mu\nu}$ which is orthogonal to u^μ (i.e. which is a 3-tensor) can be decomposed according to

$$T_{\mu\nu} = \mathcal{T} \left(r_\mu r_\nu - \frac{1}{2}s_{\mu\nu} \right) + 2\mathcal{T}_{(\mu}r_{\nu)} + \mathcal{T}_{\mu\nu}. \quad (17)$$

Here $\mathcal{T} \equiv r^\mu r^\nu T_{\mu\nu}$ is a fully radially projected 2-scalar, $\mathcal{T}^\mu \equiv s^\mu_\nu r_\lambda T^{\nu\lambda}$ is a projected 2-vector, and $\mathcal{T}^{\mu\nu} \equiv \left(s^{(\mu}_\kappa s^{\nu)}_\lambda - s^{\mu\nu} s_{\kappa\lambda}/2 \right) T^{\kappa\lambda}$ is a symmetric, trace-free 2-tensor. Any 3-vector can be similarly decomposed, although we will not need the explicit result. Any 3-scalar such as the energy density ρ is automatically also a 2-scalar.

The utility of this 1 + 1 + 2 decomposition becomes immediately apparent when we realize that, under spherical symmetry, all 2-vectors and 2-tensors must vanish. Then, with straightforward manipulations, the evolution Eqs. (11) to (14) become

$$\dot{\rho} = -\theta\rho, \quad (18)$$

$$\dot{\theta} = -\frac{\theta^2}{3} - 4\pi G\rho - \frac{3}{2}\Sigma^2, \quad (19)$$

$$\dot{\Sigma} = -\left(\frac{2}{3}\theta + \frac{1}{2}\Sigma \right) \Sigma - \mathcal{E}, \quad (20)$$

$$\dot{\mathcal{E}} = -\left(\theta - \frac{3}{2}\Sigma \right) \mathcal{E} - 4\pi G\rho\Sigma. \quad (21)$$

Here I have defined the 2-scalars $\Sigma \equiv r^\mu r^\nu \sigma_{\mu\nu}$ and $\mathcal{E} \equiv r^\mu r^\nu E_{\mu\nu}$. The set of tensorial partial differential equations, (11) to (15), has been replaced with a simple, closed set of scalar ordinary differential equations (ODEs). The magnetic Weyl tensor vanishes under spherical symmetry: no gravitational waves are possible in this case.

An equivalent way to see that all quantities reduce to 2-scalars in the spherically symmetric case is that any 3-tensor or 3-vector can only be constructed from r^μ and $s^{\mu\nu}$; no other objects are available. [Eq. (16) relates $h_{\mu\nu}$ to r_μ and $s_{\mu\nu}$.] Thus, e.g., the trace-free shear tensor $\sigma_{\mu\nu}$ must take the form

$$\sigma_{\mu\nu} = \left(r_\mu r_\nu - \frac{1}{2}s_{\mu\nu} \right) \Sigma. \quad (22)$$

C. Exact solution

The set of ODEs, Eqs. (18) to (21), could be numerically integrated, given initial conditions that satisfy the constraint equations. However, as is well known, an exact solution exists for the spherically symmetric dust spacetime [8, 9, 10]. It is normally expressed in terms of the

metric, but can be readily rewritten in terms of the covariant 2-scalars ρ , θ , Σ , and \mathcal{E} . To express the exact solution, we must first introduce a time coordinate t that labels the comoving-orthogonal slices. Because the comoving worldlines are geodesic, we can choose t to measure proper time along the worldlines; henceforth this choice will always be assumed. Similarly, it is useful to define a radial coordinate, r , which is constant along the comoving worldlines.

The result is

$$4\pi G\rho = \frac{M'}{Y^2 Y'}, \quad (23)$$

$$\theta = \frac{\dot{Y}'}{Y'} + \frac{2\dot{Y}}{Y}, \quad (24)$$

$$\Sigma = \frac{2}{3} \left(\frac{\dot{Y}'}{Y'} - \frac{\dot{Y}}{Y} \right), \quad (25)$$

$$\mathcal{E} = \frac{8\pi G}{3} \rho - \frac{2M}{Y^3}, \quad (26)$$

where $Y = Y(r, t)$ is given implicitly by

$$Y = \frac{M}{K}(1 - \cosh \eta), \quad t - t_B = \frac{M}{(-K)^{3/2}}(\sinh \eta - \eta), \quad (27)$$

and $M = M(r)$, $K = K(r) < 0$, and $t_B = t_B(r)$ are arbitrary radial functions. Here the prime symbol denotes $\partial/\partial r$. (Related solutions are known for the cases $K \geq 0$, but will not be needed here.) These expressions for the 2-scalars were first written down in [24]. Given values of t and r for which a solution is desired, and choices for the three arbitrary functions $M(r)$, $K(r)$, and $t_B(r)$, we can solve Eq. (27) for $Y(r, t)$ and its derivatives. Then we can evaluate each of Eqs. (23) to (26) to complete the solution. It is straightforward to verify explicitly that Eqs. (23) to (27) solve the ODEs (18) to (21) (as well as the initial-value constraints) for arbitrary $M(r)$, $K(r)$, and $t_B(r)$.

Because we are free to reparametrize the radial coordinate r , only *two* of the radial functions $M(r)$, $K(r)$, and $t_B(r)$ describe physically distinct solutions. Therefore, the general spherically symmetric dust solution depends on two free radial functions. It will be crucial to understand the physical significance of these two functions, which is the subject of the [appendix](#), but we can see readily from the above exact solution that as $t \rightarrow t_B(r)$, for fixed r , the density $\rho \rightarrow \infty$, i.e. we approach a physical singularity. This singularity is analogous to the initial singularity in the homogeneous and isotropic FRW space-time, but with extra radial dependence; hence the name ‘‘bang time’’ for the function $t_B(r)$.

In the [appendix](#), it is shown that the two free radial LTB functions correspond to the growing and decaying mode for linear perturbations about FRW backgrounds.

The decaying mode corresponds to fluctuations in the bang time function, $t_B(r)$, and can be set to zero by choosing $t_B(r) = \text{const}$. The growing mode corresponds to fluctuations in the spatial Ricci curvature ${}^{(3)}R$ of the comoving slices, and can be made to vanish with the choice ${}^{(3)}R = 0$. It will be very important to eliminate the decaying mode in setting up realistic void profiles, since otherwise at early times the Universe becomes extremely inhomogeneous, contradicting the standard picture of extreme post-inflationary homogeneity.

Although it will not be needed in this work, to facilitate comparison with previous studies the LTB metric can be written explicitly as

$$ds^2 = -dt^2 + \frac{Y'^2}{1-K} dr^2 + Y^2 d\Omega^2. \quad (28)$$

It reduces to the FRW metric in the homogeneous case (where the shear and electric Weyl scalars, Σ and \mathcal{E} , both vanish), and to the Schwarzschild metric outside some radius $r = L$, if $\rho(r) = 0$ for $r > L$.

III. SCALAR PERTURBATIONS ABOUT LTB BACKGROUNDS

A. Scalar-tensor coupling

The problem of evolving linear perturbations on a spherically symmetric dust (LTB) background is in principle straightforward: we must linearize the set of evolution equations (11) to (15) about an arbitrary LTB background solution. In doing so, the symmetry of the background implies that any 2-vector or 2-tensor quantities must be of first order, and hence their products can be ignored.

First consider a 2-scalar subset of the full set, namely Eqs. (11) and (12) and the contraction between $r^\mu r^\nu$ and Eqs. (13) and (14). Since we must relax (at linear order) the condition of spherical symmetry, the vector field r^μ can no longer be chosen to be exactly radial. Nevertheless, we can suppose that r^μ departs from radial only at first order. We will see in [Sec. III B](#) that 2-scalar quantities are invariant under first-order variations in the field r^μ , so we have no need to fix the field at first order. Straightforward manipulations then lead to the 2-scalar linearized set:

$$\dot{\rho} = -\theta\rho, \quad (29)$$

$$\dot{\theta} = -\frac{\theta^2}{3} - 4\pi G\rho - \frac{3}{2}\Sigma^2, \quad (30)$$

$$\dot{\Sigma} = -\left(\frac{2}{3}\theta + \frac{1}{2}\Sigma\right)\Sigma - \mathcal{E}, \quad (31)$$

$$\dot{\mathcal{E}} = -\left(\theta - \frac{3}{2}\Sigma\right)\mathcal{E} - 4\pi G\rho\Sigma + \epsilon_{\mu\nu}\nabla^\mu\mathcal{H}^\nu. \quad (32)$$

Here \mathcal{H}^ν is the 2-vector part of the $1 + 1 + 2$ decomposition of $H_{\mu\nu}$; recall Eq. (17). The symbol ∇^μ represents the sheet-projected covariant derivative, defined in analogy with Eq. (2), but with sheet projection tensors $s_{\mu\nu}$ replacing $h_{\mu\nu}$; i.e., it represents the covariant derivative in the “angular” directions. Finally, $\epsilon_{\mu\nu} \equiv \epsilon_{\mu\nu\lambda} r^\lambda$. This set of equations agrees with the corresponding linearized subset of the full set derived in [18]. Again, a set of initial-value constraint equations is not shown.

Remarkably, this set of 2-scalar equations is identical to the corresponding exact set under spherical symmetry, Eqs. (18) to (21), with the exception of the term $\epsilon_{\mu\nu}\nabla^\mu\mathcal{H}^\nu$ which couples \mathcal{E} to the magnetic Weyl tensor. Physically, this term couples scalar perturbation modes to tensor modes, represented by $H_{\mu\nu}$ [41]. While it is well known that scalars and tensors decouple when linearizing about FRW, such a coupling is expected to be a feature of the evolution on more general backgrounds, since a non-trivial background allows one to construct linear scalar quantities via, e.g., contractions between the background and tensor modes. (Recall as well that scalars couple to tensors at *second* order about FRW backgrounds, essentially since the second-order variables propagate in a nonhomogeneous first-order background.)

Unfortunately, because of the scalar-tensor coupling, the linearized set, (29) to (32), is not closed, and to complete the description of the dynamics we must include the 2-vector part of the $H_{\mu\nu}$ evolution equation, Eq. (15). This equation in turn couples to 2-vector and 2-tensor parts of the shear and electric and magnetic Weyl tensors, resulting in a very large set of equations [18]. On top of the added complexity of several more equations, the coupling to $H_{\mu\nu}$ means that we must evolve a set of *partial* differential equations. If the coupling were absent, we would only need to solve a much simpler set of *ordinary* differential equations. Indeed, as I mentioned above, in that case the set of equations would be *identical* to the corresponding set under spherical symmetry, and hence we could employ the known exact solution to those equations! (Of course, since we have ignored second-order terms in Eqs. (29) to (32), the use of the exact solution in this way could only be trusted up to first order.)

The vast simplification of the dynamics in the absence of the tensor coupling leads naturally to the question: Under what conditions could the tensor coupling be ignored to a good approximation? It is certainly reasonable to consider the case where tensors are negligible at *early* times, before the LTB background becomes nonlinear (e.g. at the time of last scattering), since many viable inflation models predict a very small primordial tensor contribution. However, even in this case, tensor modes will generally be sourced by scalars at late times, when the LTB background becomes nonlinear, according to Eq. (15).

Nevertheless, in the case of interest, namely that of linear scalar perturbations on top of a mildly nonlinear spherical inhomogeneity, it is not expected that significant tensors will be sourced. It *is* expected that tensors

would be sourced at times late enough, or scales small enough, that the scalar perturbations *themselves* have become nonlinear [25]. Essentially, nonlinear collapsing overdensities during structure formation are generically nonspherical, and hence source tensors through a significant time-dependent quadrupole moment. Instead, in the case of interest in the present work, we have *linear* fluctuations on top of a nonlinear background which itself cannot source tensor modes.

In Ref. [26], the authors performed a numerical study of the linear stability of $H_{\mu\nu} = 0$ in a few exact backgrounds, including a planar inhomogeneous Szekeres model. They found that vanishing magnetic Weyl curvature was stable during pancake collapse, but unstable during collapse towards a spindle geometry. This supports the claim that tensors can be ignored in the present context, where in the late stages of evolution of a void, the outer regions tend to collapse to form an overdense shell, which locally approximates pancake collapse geometry.

Note that dynamics with vanishing pressure and magnetic Weyl curvature are generally described by a set of ODEs along the comoving worldlines, as can be seen directly from the exact set, Eqs. (11) to (14). This was noted some time ago [27], and such a spacetime was dubbed *silent*. This name refers to the fact that without pressure and $H_{\mu\nu}$, sound waves and gravitational waves cannot be supported, respectively, and hence no direct communication can exist between neighbouring worldlines. Apart from a few special cases, such spacetimes are thought to be generally inconsistent at the nonlinear level, in that the condition $H_{\mu\nu} = 0$ imposes a new constraint on the dynamics which is not consistent with the remaining dynamical equations [28]. However, in the present context we are only assuming that the coupling to tensors can be ignored at linear order. Also, we do not require that the full tensor $H_{\mu\nu}$ vanish, only the weaker condition that $\epsilon_{\mu\nu}\nabla^\mu\mathcal{H}^\nu$ can be ignored.

Henceforth I will assume that the tensor coupling term can be ignored in Eq. (32) in evolving perturbations on LTB backgrounds. As a consistency check, I show in Section IV that for a particular LTB profile chosen to provide a rough fit to the luminosity distance-redshift relation of standard Λ cold dark matter (Λ CDM) models, the background shear, through which tensors must couple to density perturbations, only very weakly affects the density perturbations. Such a test should be performed for any such calculation of scalar perturbations on LTB backgrounds. Obviously the full set of equations, including tensors, could in principle be evolved to check the validity of the weak tensor-scalar coupling approximation. This might be necessary if we were interested in evolving perturbations on spherical *overdensities* at the late stages of collapse, instead of underdensities.

B. Defining perturbations

The dynamical equations derived in Section III A describe the evolution of the *total* quantities ρ , θ , Σ , and \mathcal{E} , i.e. backgrounds plus perturbations, in the linear approximation. For many purposes it is very useful to obtain the evolution of appropriately defined perturbations alone. To do this in the metric-based approach to perturbation theory, one first provides a mapping (i.e. makes a gauge choice) between the real spacetime and a fictitious background (usually FRW). Perturbations in any quantity are then defined as the difference between the exact value at some event and the background value mapped to that event. The freedom to vary the mapping results in the familiar gauge ambiguity.

On the other hand, within the 1+3 covariant approach to perturbation theory (see [19] for a recent review) perturbations are usually represented by spatial *gradients* orthogonal to the timelike direction u^μ ; e.g., density fluctuations are characterized by the 3-vector $D_\mu\rho$. The intention is to describe fluctuations in a gauge-invariant and covariant manner. However, it is easy to see that precisely the same ambiguity exists in this approach as in the metric approach. If we choose u^μ to be orthogonal to hypersurfaces of constant energy density, then we have $D_\mu\rho = 0$ trivially, i.e. we have “gauged away” the density perturbation. Of course, as we have seen here, in the case of a single-component matter source, there is a natural choice for u^μ which simplifies the dynamical equations, namely the comoving choice. But this choice is not necessary.

While the ability to define perturbations entirely within the true spacetime is an advantage of the covariant approach for FRW backgrounds, it does not appear to be possible to extend this approach to LTB backgrounds. This is because, on the natural comoving-orthogonal slices, gradients such as $D_\mu\rho$ do not generally vanish at *background* level, and hence they cannot be said to characterize the perturbations alone. Therefore, here I will employ a more standard approach, defining the density perturbation as the difference

$$\delta\rho(x^\mu) \equiv \rho(x^\mu) - \rho^{(0)}(r, t). \quad (33)$$

Here $\rho(x^\mu)$ is the density at event x^μ in the true, perturbed spacetime, and $\rho^{(0)}(r, t)$ is the density at the corresponding event in the background, in this case a spherically symmetric LTB spacetime. I define perturbations in the 2-scalars θ , Σ , and \mathcal{E} analogously. The comoving worldlines in a dust spacetime provide a natural choice for the time coordinate. This coordinate is chosen (in both true and background spacetimes) such that hypersurfaces of constant t are orthogonal to the comoving worldlines, and t measures proper time along those worldlines. This fixes the “temporal gauge.”

There is inevitable freedom in choosing the radial coordinate r , since no radial vector r^μ is naturally defined in the perturbed spacetime, and there is no unique notion of distance in a curved spacetime. We can defeat this

ambiguity by considering the intended application of the perturbed LTB formalism, namely the evolution of linear scalar perturbations on top of a spherical void. Such a void becomes nonlinear at late times, but, as discussed in the [appendix](#), must consist of a pure growing mode, to be consistent with the inflationary paradigm. Hence the spacetime approaches FRW plus linear perturbations at early times (such as the time of last scattering). We can define r in the FRW background at such early times to give radial proper distance from some centre. Then we can define r on the perturbed spacetime at early times to be *any* radial coordinate that agrees, to first order, with the background radial coordinate. Taking the background at this early time to be homogeneous FRW, any *linear* variations $r \rightarrow r + \delta r$ in the radial coordinate *cannot* affect the values of any perturbed physical quantities, to first order. (*Physical* perturbations in FRW are invariant under purely *spatial* gauge transformations, at first order [29, 30].) We then define r at later events such that it is constant along each comoving worldline in the true spacetime, i.e. r is “dragged” along by the fluid flow. (Therefore comoving worldlines in the background are mapped to comoving worldlines in the perturbed spacetime.) The spacelike vector field r^μ is defined to be normal to surfaces of constant r . These surfaces will be linearly perturbed versions of 2-spheres.

Note that a type of radial gauge dependence may be present in perturbations at late times. In regions where the background energy density, e.g., has a significant spatial gradient, it may be possible to gauge away a density perturbation $\delta\rho$ with a radial gauge transformation. (Indeed this gauge dependence may continue to early times if we consider the background to be LTB, rather than FRW, at the early times.) However, we will not be able to gauge away $\delta\rho$ everywhere, since the density gradient will not be large everywhere ($d\rho/dr$ must vanish at the origin if ρ is to be smooth there). In the FRW case, the usual monotonicity of the background $\rho(t)$ does allow us to set $\delta\rho = 0$ everywhere. The possible gauge dependence in the LTB case must be kept in mind when interpreting the results of calculations. Of course, a calculation of any *observable* quantity must be independent of any gauge choice. [An example would be the variance of $\delta\rho$ across a 2-sphere of constant redshift (which is directly observable), rather than some arbitrary coordinate r (which is not).]

Recall that in the 1 + 1 + 2 formalism, 2-scalars are constructed from 3-vectors or 3-tensors by fully projecting along r^μ . Thus we might be concerned that linear variations in r^μ , which will necessarily follow from linear variations in the coordinate r , might change the values of 2-scalars, at least at late times when the background has become nonlinear. However, this does not happen, *at first order*, because of the isotropy of the background. Consider an exact, spherically symmetric LTB background, with exactly radial vector r^μ and linearly perturbed vector

$$\tilde{r}^\mu \equiv r^\mu + \delta r^\mu. \quad (34)$$

Imposing the normalization $\tilde{r}^\mu \tilde{r}_\mu = 1$ gives $\tilde{r}^\mu r_\mu = 1 + \mathcal{O}(2)$. Therefore, defining the shear scalar Σ using the radial r^μ , $\Sigma \equiv r^\mu r^\nu \sigma_{\mu\nu}$, we have

$$\tilde{\Sigma} \equiv \tilde{r}^\mu \tilde{r}^\nu \sigma_{\mu\nu} = \Sigma + \mathcal{O}(2). \quad (35)$$

(A similar result applies to the electric Weyl tensor.) That is, linear variations in r^μ do not affect the values of 2-scalars, to first order. Clearly the presence of perturbations will not change this result, since the variations in the values of 2-scalars due to the presence of linear perturbations as r^μ is varied at first order will also be of at least second order.

To summarize, the temporal gauge is chosen to be comoving, while the radial gauge is any linear variation about “initial slice proper distance gauge.” The temporal choice simplifies the dynamical equations, while the radial choice enables the simple adaptation of standard results from the theory of perturbations on FRW backgrounds, as we will see in Sec. III E.

C. LTB transfer functions

Inserting the definition of $\delta\rho$, Eq. (33), and the corresponding expressions for the other 2-scalar perturbations, into the linearized set, Eqs. (29) to (32) (dropping the tensor coupling), and discarding terms quadratic in the perturbations, we obtain

$$\delta\dot{\rho} = -\theta\delta\rho - \rho\delta\theta, \quad (36)$$

$$\delta\dot{\theta} = -\frac{2}{3}\theta\delta\theta - 4\pi G\delta\rho - 3\Sigma\delta\Sigma, \quad (37)$$

$$\delta\dot{\Sigma} = -\left(\frac{2}{3}\theta + \Sigma\right)\delta\Sigma - \frac{2}{3}\Sigma\delta\theta - \delta\mathcal{E}, \quad (38)$$

$$\begin{aligned} \delta\dot{\mathcal{E}} = & -\left(\theta - \frac{3}{2}\Sigma\right)\delta\mathcal{E} - \mathcal{E}\left(\delta\theta - \frac{3}{2}\delta\Sigma\right) \\ & - 4\pi G(\rho\delta\Sigma + \Sigma\delta\rho). \end{aligned} \quad (39)$$

In obtaining these equations, the fact that comoving worldlines in the background are mapped to comoving worldlines in the perturbed spacetime has allowed us to subtract off the background equations of motion, Eqs. (18) to (21). Also, note that it is valid to trivially perturb time derivatives (e.g., $\delta\dot{\rho} = \dot{\rho} - \dot{\rho}^{(0)}$), since t measures proper time in both background and perturbed spacetimes.

In a sense, this completes the problem of perturbations on LTB backgrounds, since the set of ODEs, Eqs. (36) to (39), can be readily solved numerically (or even using the exact solution from Sec. II C, remembering that that solution can only be trusted to linear order here). However, with applications in mind, it will be very useful to

develop a description of the evolution of the perturbations in terms of a new set of *transfer functions*. This will allow us to derive results that parallel remarkably closely the standard results from perturbation theory on FRW.

Consider the column vector of 2-vector perturbations, $\delta X_i(t, r, n^\mu)$, where $X_i = \rho, \theta, \Sigma, \mathcal{E}$. Here n^μ is the spatial unit vector from the origin, $r = 0$, towards the point at which δX_i is evaluated, so (r, n^μ) are the polar coordinates of that point. Then the linear perturbations at some arbitrary time t must be related to those at some initial time t_i via the matrix product

$$\delta X_i(t, r, n^\mu) = T_{ij}(t, r)\delta X_j(t_i, r, n^\mu), \quad (40)$$

where $T_{ij}(t, r)$ is a 4×4 matrix of transfer functions. Linearity of evolution demands that Eq. (40) take a linear form. The property of “silence,” i.e. that the perturbations are solutions of ODEs, means that the solution at event (t, r, n^μ) can only depend on the initial condition on the same worldline at (t_i, r, n^μ) . (Initial velocities $\delta\dot{X}_i$ are not needed since the ODEs are first order.) Finally, the isotropy of the background implies that the transfer functions T_{ij} must depend only on t and r .

In the case of perturbations on FRW, the corresponding transfer functions are generally scale (i.e. k) dependent, although this is only true when pressure is present to support acoustic waves and introduce spatial derivatives into the dynamical equations. In the LTB case here, no such scale dependence exists. Also, the FRW transfer functions appear to be considerably simpler than their LTB counterparts, in that they depend on t alone in the homogeneous case. However, again with applications in mind, we will very often be interested in evaluating the perturbations on the observer’s past light cone (with the observer located at the centre of symmetry). The surface of that cone defines a definite relationship $r = r(t)$ (at background order), and so the LTB transfer functions can in practice be considered to be functions of the time alone, $T_{ij}(t, r) = T_{ij}(t, r(t))$.

Thus the problem of linear perturbations on LTB backgrounds, which at first may have appeared quite daunting, is reduced to that of calculating a small number of transfer functions of a single variable, for most practical applications. As we will see next, the problem can be simplified even further by consideration of the initial conditions.

D. Initial conditions

In order to use Eq. (40) to evolve the perturbations we must first specify initial conditions. To do this, first recall again the context in which we are considering LTB backgrounds here. We require growing mode solutions, which approach linearly perturbed FRW at early times. Therefore, we can set up initial conditions for the fluctuations at some sufficiently early time t_i , exactly as in

the standard FRW case. For definiteness (and well supported by current observations [31]), I will assume that the primordial fluctuations are scalar and adiabatic. In addition, with their inflationary origin in mind, I will take the perturbations at the initial time, t_i , to be purely in the growing mode (this assumption is also supported by the observations [32]). Since the above calculations have assumed vanishing pressure, we must take the initial time for the specification of perturbations to be sufficiently late that matter domination is a good approximation.

With these assumptions, we can reduce the number of LTB transfer functions that need to be calculated, since some of the initial perturbations can be written in terms of the others. It will be particularly useful to write all of the initial perturbations in terms of the comoving curvature perturbation, $\mathcal{R}(x^\mu)$. This quantity is constant on super-Hubble scales (for adiabatic modes), and hence is very convenient for comparing with the predictions of a particular inflationary model. Constraints on the primordial value of \mathcal{R} are also explicitly provided in observational results (see, e.g., [31]).

During matter domination, the comoving energy density perturbation can be written in terms of \mathcal{R} as

$$\frac{\delta\rho}{\rho} = -\frac{18}{5} \frac{D^2}{\theta^2} \mathcal{R} \quad (41)$$

(see, e.g., [33]), where $D^2 \equiv D^\mu D_\mu$ is the spatial Laplacian. At the initial time t_i , the shear tensor for scalar fluctuations can be derived from a scalar function $\sigma(x^\mu)$, according to

$$\sigma_{\mu\nu} = D_\mu D_\nu \sigma - \frac{1}{3} h_{\mu\nu} D^2 \sigma. \quad (42)$$

Again during matter domination, the comoving shear scalar σ can be written in terms of the comoving curvature perturbation as

$$\sigma = \frac{6}{5} \frac{\mathcal{R}}{\theta} \quad (43)$$

(see, e.g., [30]). Combining these results we can write for the shear 2-scalar initial condition at t_i ,

$$\frac{\delta\Sigma}{\theta} = \frac{r^\mu r^\nu \sigma_{\mu\nu}}{\theta} = \frac{6}{5} \frac{1}{\theta^2} \left(\frac{\partial^2}{\partial r^2} - \frac{1}{3} D^2 \right) \mathcal{R}. \quad (44)$$

Note that, even though both $\delta\rho$ and $\delta\Sigma$ are completely determined by the comoving curvature \mathcal{R} , they are not simply proportional. Geometrically, it is possible, e.g., that some localized linear fluctuation in \mathcal{R} produces a $\delta\rho$ at some point, but no $\delta\Sigma$, if the fluctuation is symmetric about the point. Nevertheless, in the [appendix](#), Eqs. (A.1) and (A.2) show that the growing modes for the comoving gauge energy density and expansion perturbations are related by

$$\frac{\delta\rho}{\rho} = -3 \frac{\delta\theta}{\theta}. \quad (45)$$

Similarly, using Eq. (38) (for the relevant case at t_i that the background shear Σ is first order and hence can be dropped from this equation) and Eq. (44), we can relate the electric Weyl 2-scalar to the shear via

$$\delta\mathcal{E} = -\frac{1}{2} \theta \delta\Sigma. \quad (46)$$

It is important to point out that these initial conditions must automatically satisfy the Einstein initial-value constraint equations, to linear order. Hence all that remains is to determine the transfer functions to evolve the initial conditions.

The proportionalities (45) and (46) apply at the initial time, t_i , and hence they reduce the dimensionality of the matrix of transfer functions in Eq. (40) to 2×2 . For example, the evolution of the density perturbation is given by

$$\begin{aligned} \frac{\delta\rho(t, r, n^\mu)}{\rho(t, r)} &= T_{\rho\rho}(t, r) \frac{\delta\rho(t_i, r, n^\mu)}{\rho(t_i)} \\ &\quad - T_{\rho\Sigma}(t, r) \frac{3\delta\Sigma(t_i, r, n^\mu)}{\theta(t_i)}, \end{aligned} \quad (47)$$

and we only need to calculate two transfer functions. In this expression I have scaled the perturbations so that the transfer functions are dimensionless and positive, and the function $T_{\rho\rho}$ approaches unity at early times ($T_{\rho\Sigma}$ approaches zero at early times).

E. Harmonic decomposition

One of the difficulties that comes to mind when first considering the problem of linear perturbations on LTB backgrounds is that of harmonic expansion. A crucially important tool in perturbation theory on flat FRW backgrounds is the ability to expand fluctuations in Fourier modes or spherical harmonics and spherical Bessel functions. This approach can be generalized to the case of spatially curved FRW backgrounds. But an LTB background can have an *arbitrary* radial dependence of the spatial curvature, so it appears hopeless to look for radial harmonics generally (although the standard spherical harmonic functions, the $Y_{\ell m}$'s, can be used to expand the angular dependence, of course).

Again, though, we are considering spacetimes which approach linearly perturbed FRW at early times. Therefore we should be able to employ the usual harmonic expansions *at a sufficiently early time*. Then we can evolve the perturbations using the transfer functions introduced in Section III C. The use of standard harmonic expansions at early times will, e.g., allow us to answer statistical questions about the perturbations at late times, using the standard formalism of Gaussian random fields, just as we do on FRW backgrounds.

To see how this works explicitly, consider first the comoving curvature perturbation \mathcal{R} . At the initial time t_i ,

when the fluctuations are well described by linear perturbations from FRW, we can expand \mathcal{R} in spherical harmonics as

$$\mathcal{R}(t_i, r, n^\mu) = \sqrt{\frac{2}{\pi}} \int dk k \sum_{\ell m} \mathcal{R}_{\ell m}(k, t_i) j_\ell(kr) Y_{\ell m}(n^\mu), \quad (48)$$

where j_ℓ is a spherical Bessel function of the first kind and k is a comoving wave number. The curvature perturbation \mathcal{R} evaluated at time t_i , during matter domination, is related to the *primordial*, constant value \mathcal{R}^{pr} via the standard matter transfer function $T(k)$:

$$\mathcal{R}_{\ell m}(k, t_i) = T(k) \mathcal{R}_{\ell m}^{\text{pr}}(k) \quad (49)$$

(see, e.g., [33]). The function $T(k)$ describes the suppres-

sion of power in \mathcal{R} incurred while each mode is inside the Hubble radius during radiation domination. Assuming Gaussian random primordial fluctuations, the statistics of \mathcal{R}^{pr} are entirely encoded in the standard expression

$$\langle \mathcal{R}_{\ell m}^{\text{pr}}(k) \mathcal{R}_{\ell' m'}^{\text{pr}*}(k') \rangle = 2\pi^2 \frac{\mathcal{P}_{\mathcal{R}}(k)}{k^3} \delta(k - k') \delta_{\ell\ell'} \delta_{mm'}. \quad (50)$$

Here the angled brackets indicate averaging over the ensemble of realizations of the fluctuations. For a scale invariant primordial spectrum the dimensionless power spectrum $\mathcal{P}_{\mathcal{R}}(k)$ is constant.

Taking the energy density as an example, by combining Eqs. (41), (44), and (47) to (49), we can write

$$\frac{\delta\rho(t, r, n^\mu)}{\rho(t, r)} = \frac{2}{5} \sqrt{\frac{2}{\pi}} \int dk k T(k) \sum_{\ell m} \mathcal{R}_{\ell m}^{\text{pr}}(k) T_\rho(t, r, k, \ell) Y_{\ell m}(n^\mu), \quad (51)$$

where I have defined a new transfer function by

$$T_\rho(t, r, k, \ell) \equiv \left(\frac{k}{a_i H_i} \right)^2 \left[T_{\rho\rho}(t, r) j_\ell(kr) - T_{\rho\Sigma}(t, r) \left(j_\ell''(kr) + \frac{1}{3} j_\ell(kr) \right) \right]. \quad (52)$$

Here I have explicitly included the scale factor a_i at time t_i , and $H_i \equiv \theta(t_i)/3$. The notation j_ℓ'' indicates the second derivative of j_ℓ with respect to its argument. Note that the details of a particular void profile enter these expressions only through the LTB transfer functions $T_{\rho\rho}(t, r)$ and $T_{\rho\Sigma}(t, r)$. I stress that the decomposition into wave numbers k in these expressions has been done at the early time t_i , so the harmonic expansion is valid.

We can now calculate any statistical aspect of the $\delta\rho$ field, at any time. For example, consider the angular power spectrum of density fluctuations on a sphere of some particular radius r and at some particular time t , defined by

$$C_\ell^{\delta\rho}(t, r) \equiv \left\langle \int \frac{\delta\rho(t, r, n^\mu)}{\rho(t, r)} Y_{\ell m}^*(n^\mu) d\Omega \right\rangle^2 \quad (53)$$

[presumably $r = r(t)$ if we are interested in observations on the past light cone]. Using Eqs. (50) and (51), and the orthonormality property of the spherical harmonics, we can evaluate this expression as

$$C_\ell^{\delta\rho}(t, r) = \frac{16\pi}{25} \int \frac{dk}{k} T^2(k) T_\rho^2(t, r, k, \ell) \mathcal{P}_{\mathcal{R}}(k). \quad (54)$$

Using similar techniques we can calculate a large variety of observable quantities, which allows us to confront void models of acceleration with observations at the level of perturbations [21].

IV. NUMERICAL EVOLUTION

It is now a straightforward exercise to calculate any of the LTB transfer functions defined above. First, we must specify an LTB background about which to perturb. For numerical convenience I have used the function $K(r)$ defined in Sec. II C to specify the initial profile, using the exact solution, Eqs. (23) to (27). As discussed in the appendix, I have set the bang time function $t_B(r)$ to zero to eliminate the decaying mode. The remaining radial gauge freedom was used to set $M(r) = r^3$, which is the value the corresponding function would take in FRW; although as discussed in Sec. III B any choice of radial coordinate that agrees with the background at zeroth order would do.

For the initial profile I chose

$$K(r) = \begin{cases} K_m \left[\left(\frac{r}{L} \right)^5 - \frac{9}{5} \left(\frac{r}{L} \right)^4 + \left(\frac{r}{L} \right)^2 \right], & r \leq L, \\ \frac{1}{5} K_m \frac{L}{r}, & r > L. \end{cases} \quad (55)$$

This profile is characterized by two parameters, a width L and an amplitude K_m . For $r \gg L$, it approaches flat, matter-dominated FRW, i.e. the Einstein-de Sitter (EdS) universe. I chose units such that the initial time was $t_i = 1$, and an amplitude which gave a spatial curvature of $({}^{(3)}R/\theta^2) = -5.5 \times 10^{-4}$ at t_i , so that the initial profile is

a small perturbation from FRW. The profile was chosen to roughly fit the luminosity distance-redshift relation for standard Λ CDM models, while providing a reasonable density parameter Ω_m today. However, evaluating the goodness of fit of the current LTB model to data is beyond the scope of this paper, and will be the subject of a future detailed study [21].

In Fig. 1, I display the background profiles for the energy density, expansion rate, 2-scalar shear, and spatial curvature ${}^{(3)}R$ calculated from the linearized Einstein energy constraint equation,

$$\frac{\theta^2}{3} = 8\pi G\rho - \frac{1}{2}{}^{(3)}R + \frac{3}{4}\Sigma^2. \quad (56)$$

All quantities are displayed at the late time $t = 1.0 \times 10^5$, and were calculated using the exact solution, Eqs. (23) to (27). In the plot, the expansion and shear 2-scalar are normalized by the value of the expansion rate at the origin, θ_{\max} . The energy density and spatial curvature are normalized such that their difference should be unity, according to Eq. (56) (the shear squared term is small compared to the density and curvature).

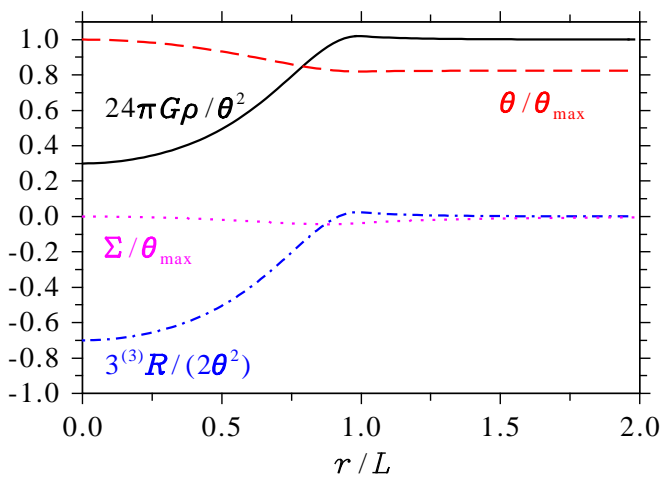


FIG. 1: Background LTB radial profile at the late time $t = 1.0 \times 10^5$. Energy density ρ , volume expansion rate θ , shear 2-scalar Σ , and spatial curvature ${}^{(3)}R$ are scaled as described in the text. This profile corresponds to an underdensity near the origin with effective density and curvature parameters $\Omega_m = 0.3$ and $\Omega_K = 0.7$.

Note that the normalized energy density and spatial curvature plotted in Fig. 1 correspond directly to the FRW definitions of the matter and (negative of the) curvature parameters, Ω_m and Ω_K . Therefore we can see that this LTB profile corresponds, at the late time plotted, to a significant underdensity extending from the centre to $r \simeq L$, with effective density and curvature parameters $\Omega_m = 0.3$ and $\Omega_K = 0.7$ at the centre. Corresponding to this underdensity is a higher expansion rate than the asymptotic flat region. The shear is small except at the boundary region $r \sim L$; it must vanish at the centre and in the asymptotic FRW region by symmetry.

Figure 2 shows the transfer functions $T_{\rho\rho}$ and $T_{\rho\Sigma}$, which determine the evolution of the density perturbation according to Eq. (47). They were calculated by numerically evolving the linearized set, Eqs. (36) to (39). They have been normalized via

$$T_{\rho\rho}^{\text{norm}}(t, r) \equiv \left(\frac{t_i}{t}\right)^{2/3} T_{\rho\rho}(t, r), \quad (57)$$

and similarly for $T_{\rho\Sigma}$. This normalization was chosen so that, for the EdS case, $T_{\rho\rho}^{\text{norm}}(t) = 1$ [and $T_{\rho\Sigma}^{\text{norm}}(t) = 0$] for all time. The transfer functions are shown at the logarithmically-spaced times $t = 46.4$, 2154 , and 1.0×10^5 .

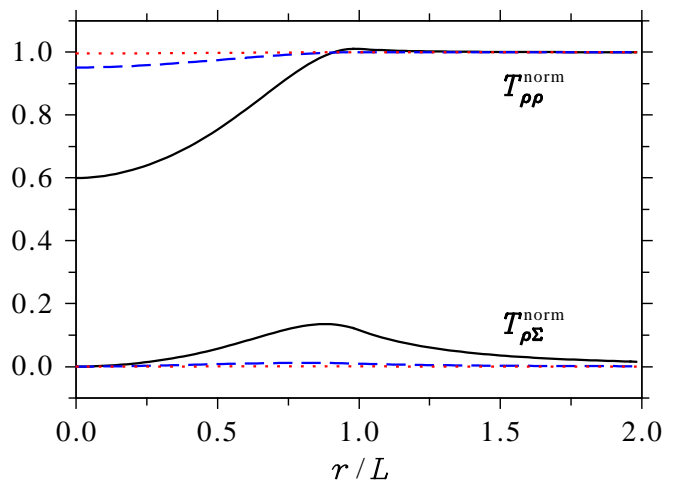


FIG. 2: Transfer functions $T_{\rho\rho}$ and $T_{\rho\Sigma}$, normalized so that $T_{\rho\rho}^{\text{norm}} = 1$ at all times for an Einstein-de Sitter background. The functions are presented for the times $t = 46.4$ (red, dotted line), $t = 2154$ (blue, dashed line), and $t = 1.0 \times 10^5$ (black, solid line). Significant suppression of perturbations occurs at late times within the void, and density perturbations are also sourced by shear fluctuations at late times through $T_{\rho\Sigma}$.

We can see from Fig. 2 that at early times, and for $r \gg L$, the transfer functions approach their EdS values. That is, the density perturbation is evolving as expected when the background is (locally) nearly EdS. However, we see a significant suppression in the growth of density perturbations at late times within the void. This suppression has an intuitive origin: near the centre of the void, the spacetime approximates the open FRW geometry, for which it is known that the growth of structure is suppressed compared with EdS (see, e.g., [33]). It is possible to verify that the amount of suppression at the origin quantitatively matches the open FRW prediction [21].

The function $T_{\rho\Sigma}$ plotted in Fig. 2 illustrates that, at late times in the nonlinear background regime, shear fluctuations can source density fluctuations, via coupling through the background shear [recall Eqs. (36) and (37)]. The importance of this effect is not clear from this figure, however, since the two transfer functions $T_{\rho\rho}$ and

$T_{\rho\Sigma}$ multiply different combinations of Bessel functions in Eq. (52).

Finally, Fig. 3 illustrates the transfer function $T_\rho(t, r, k, \ell)$, which was defined in Eq. (52), again normalized according to

$$T_\rho^{\text{norm}}(t, r, k, \ell) \equiv \left(\frac{t_i}{t}\right)^{2/3} T_\rho(t, r, k, \ell), \quad (58)$$

for the case $\ell = 10$ (the general features are very similar for other values of ℓ). With this normalization, we have $T_\rho(t, r, k, \ell) = (k/a_i H_i)^2 j_\ell(kr)$ for all t and r for the special case of the EdS universe, and this case is plotted in Fig. 3. Also plotted are the curves for the LTB model defined above, and evaluated within the periphery of the void, at $r/L = 0.7$, and near the void centre, at $r/L = 0.01$ (cf. Fig. 2). For the LTB cases, the transfer function is evaluated on the past light cone. Figure 3 illustrates again the suppression of matter fluctuations near the origin with respect to the EdS case.

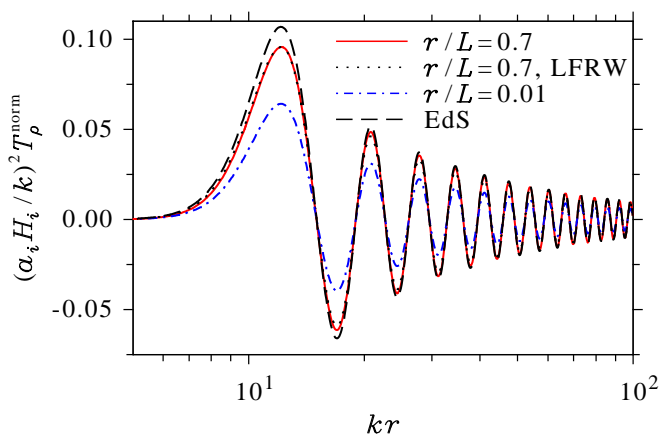


FIG. 3: Normalized transfer function $T_\rho^{\text{norm}}(t, r, k, \ell)$ for $\ell = 10$. The curves are shown for a point within the periphery of the LTB void, at $r/L = 0.7$, as well as near the void centre at $r/L = 0.01$. Also shown is the local FRW approximation (LFRW) for $r/L = 0.7$, together with the Einstein-de Sitter case (EdS).

To illustrate the effect of the background shear Σ and tidal field \mathcal{E} , which are non-negligible only within the peripheral region of the void (recall Fig. 1), Fig. 3 also presents the transfer function $T_\rho(t, r, k, \ell)$ evaluated at $r/L = 0.7$, but calculated by ignoring the background shear and tidal field in the linearized evolution Eqs. (36) to (39). This approximation can be called the “local FRW approximation,” since setting $\Sigma = \mathcal{E} = 0$ results in the evolution of the local quantities (background and perturbations) along each worldline that is identical to that of some FRW universe. We see that the local FRW approximation is very good, even in the void periphery, where the background shear and tidal field are largest. (The local FRW approximation transfer function for $r/L = 0.01$ is indistinguishable from the corresponding curve plotted in Fig. 3.) Note that in the local FRW

approximation we have $T_{\rho\Sigma} = 0$, so Fig. 3 shows that modifications to the matter power spectrum due to shear fluctuations (as encoded in the transfer function $T_{\rho\Sigma}$) are subdominant to the main suppression which is captured well by the local FRW approximation.

Recall that the tensor modes, which we have ignored in all of these calculations, couple to $\delta\rho$ only through the shear [see Eqs. (29) to (32)]. Since the magnitude of the background shear does not depend on the amplitude of linear tensor perturbations, the weak effect of the shear that we have observed (i.e. the excellent accuracy of the local FRW approximation) means that it is very unlikely that the tensors would have a significant effect on the density fluctuations had the tensors been included. It should be stressed that this result will depend on the background profile: a background more strongly nonlinear, and hence with larger shear, than the one studied here will couple both scalar shear fluctuations and tensor modes more strongly to the density perturbations. Thus the importance of the background shear should be evaluated whenever evolving scalar perturbations on an LTB background. As well, the effect of the background shear may be larger on quantities other than the density perturbations.

V. DISCUSSION

It is expected that the formalism developed here could be applied to constraining void models for acceleration with a wide variety of structure-related data. Such a program could perhaps be dubbed “testing homogeneity with inhomogeneities.” Examples include the shape (and amplitude) of the local matter power spectrum, a rigorous treatment of baryon acoustic oscillations, and the effects of gravitational lensing by linear structures. These applications are currently under study [21]. Apart from void models, it is expected that the present approach could find use elsewhere, in particular in examining the early stages of the standard structure formation process.

A particularly interesting application would be a full calculation of the effects of a void inhomogeneity on the CMB. The effect of varying the angular diameter distance to the last scattering surface in standard FRW cosmologies is a change in the angular peak scale (indeed, this is the dominant effect on the spectrum from varying the *time* of observation, keeping everything else fixed [34]), which can already be calculated at background level in LTB models [11]. The free-streamed primary CMB anisotropy power spectrum is expected to be very robust to the presence of isotropic inhomogeneity. However, recall from Fig. 2 that the presence of a large nonlinear void results in a *suppression* of the power of scalar fluctuations inside the void. Such a suppression exists at late times in standard Λ CDM models (as well as in open models), where it leads to the integrated Sachs-Wolfe (ISW) effect. An analogous effect should occur in void models, which will provide another handle on constraining these models.

The ISW effect modifies the largest angular scales, and so its presence is difficult to distinguish directly due to cosmic variance. However, correlations with large-scale structure have been measured with high confidence [35], and this is a signature that the present formalism could be used to calculate for void models. Even if the overall *amplitude* of the ISW-structure correlations turns out to be insufficiently constraining, it would be very surprising if the redshift-dependence of the effect would be similar between void and Λ CDM models.

It is important to stress again that the present approach is grounded within the well-developed theory of linear perturbations on FRW backgrounds, and many of the familiar standard techniques from that field can be applied here. The main difference is the presence of a small number of new, simple to calculate linear transfer functions. In practical terms, these transfer functions only need to be calculated once for a particular void profile, and can be expressed as a function of a single variable if results are required on the past light cone, as is normally the case. This connection with standard FRW perturbation theory was made possible by the crucial assumption that voids contain no decaying modes, so that they are consistent with the early homogeneity predicted by models of inflation.

On the theoretical side, future work could include the calculation of the remaining 2-vector and 2-tensor shear and electric Weyl degrees of freedom, which, in the absence of coupling to $H_{\mu\nu}$, also evolve according to ODEs, as Eqs. (13) and (14) show. Apart from possible observational consequences of these components, this would enable a consistency check on the accuracy of ignoring the tensor coupling by monitoring the irrotational constraint equation [19]

$$H_{\mu\nu} = \text{curl}\sigma_{\mu\nu}. \quad (59)$$

However, it is important to stress that, for the void model studied here, the effect of the background shear on the density fluctuations was found to be weak. Thus any tensors produced are not expected to have a significant effect on the density perturbations. The dominant effect, namely a significant suppression of power within the void, was found to be captured well by the local FRW approximation, which ignores the background shear and tidal field. Crucially, this dominant suppression near the origin is independent of the details of the void profile away from the origin, since the background shear must vanish at the origin by isotropy, so that the local FRW approximation is exact there. Similarly, the degree of suppression near the centre will not be affected by tensors, which require background shear to couple to density fluctuations.

To conclude, proponents for void scenarios argue that they are conservative in that they require no new, mysterious dark energy component (although, of course, they leave the solution of the cosmological constant problem to future work!), and that they may naturally explain the ‘‘coincidence problem,’’ since structure started to go

nonlinear only recently. Ultimately, though, we will need to resort to the widest range of observations possible to determine if the apparently natural philosophical stance of the Copernican principle actually reflects our place in the Universe.

Acknowledgments

This research was supported by the Natural Sciences and Engineering Research Council of Canada. I thank Adam Moss and Douglas Scott for useful discussions.

APPENDIX: GROWING AND DECAYING MODES

1. Linearized FRW solution

We saw in Sec. IIC that the general spherically symmetric dust (LTB) spacetime is specified by two free radial functions. To help elucidate the physical significance of these two free functions, consider an LTB spacetime which is very ‘‘close’’ to FRW, in the sense that it can be treated as a linear perturbation from FRW. It is well known from the theory of cosmological perturbations (see, e.g., [36]) that a general linear dust perturbation on FRW is described by two modes, one growing and one decaying. [This can be seen easily from the exact Eqs. (11) and (12): For an FRW background, the shear term $\sigma_{\mu\nu}\sigma^{\mu\nu}$ is second order, and hence the linearized Eqs. (11) and (12) decouple from the remaining evolution equations and form a second order system with two independent solutions.] Therefore we can conclude that the two free functions of an LTB spacetime correspond to growing and decaying modes in the linear regime about FRW. This point was made some time ago in Ref. [37] (see also [38]), but it will be useful to derive the result here in a more explicit manner.

The importance of this result is that the presence of a significant decaying mode at *late* times will result in extreme inhomogeneity at *early* times, contradicting the standard inflationary scenario, according to which the Universe is expected to be extremely homogeneous at the end of inflation. Hence we will need to know how to set the decaying mode to zero in setting up a spherical LTB profile. This reduces the freedom available in choosing a profile, and hence should make it more difficult to fit all of the data.

The evolution of the *comoving gauge* dust energy density perturbation $\delta\rho$ in a pressureless FRW background is given by

$$\frac{\delta\rho}{\rho} = \left(\frac{t}{t_0}\right)^{2/3} D_1(x) + \frac{t_0}{t} D_2(x), \quad (\text{A.1})$$

where $D_1(x)$ and $D_2(x)$ are the amplitudes of the growing and decaying modes, respectively, and t_0 is an arbitrary

reference time. [It is straightforward to show that this expression is the solution to the linearized Eqs. (11) and (12).] Similarly, it can be shown that the comoving gauge expansion perturbation $\delta\theta$ [42] is given by a growing and decaying mode,

$$\frac{\delta\theta}{\theta} = -\frac{1}{3} \left(\frac{t}{t_0}\right)^{2/3} D_1(x) + \frac{1}{2} \frac{t_0}{t} D_2(x). \quad (\text{A.2})$$

Using these two expressions and the linearized energy constraint equation, we can show that the 3-Ricci curvature of the comoving slices, ${}^{(3)}R$, evolves according to

$$-\frac{3}{2} \frac{{}^{(3)}R}{\theta^2} = -\frac{5}{3} \left(\frac{t}{t_0}\right)^{2/3} D_1(x). \quad (\text{A.3})$$

Note that the curvature perturbation consists of *just the growing mode*. The normalization of the 3-curvature perturbation in Eq. (A.3) has been chosen to agree with the conventional FRW curvature parameter,

$$\Omega_K = -\frac{3}{2} \frac{{}^{(3)}R}{\theta^2} \quad (\text{A.4})$$

in the homogeneous limit.

2. Vanishing growing mode

I showed above that a comoving 3-curvature perturbation corresponds to a pure *growing* mode in linear theory on an FRW background. Therefore we can isolate the *decaying* mode by considering solutions with vanishing spatial Ricci curvature ${}^{(3)}R$. For an LTB spacetime which is a small perturbation from FRW, the exact energy conservation and Raychaudhuri equations, (11) and (12), become, to first order,

$$\dot{\rho} = -\theta\rho, \quad (\text{A.5})$$

$$\dot{\theta} = -\frac{\theta^2}{3} - 4\pi G\rho, \quad (\text{A.6})$$

since the shear $\sigma_{\mu\nu}$ is a first-order quantity. Under the same approximation, the Einstein energy constraint equation becomes

$$\frac{\theta^2}{3} = 8\pi G\rho - \frac{1}{2} {}^{(3)}R. \quad (\text{A.7})$$

For the case ${}^{(3)}R = 0$, it is simple to verify that the solution to these equations is

$$\rho(r, t) = \frac{1}{6\pi G[t - t_B(r)]^2}, \quad (\text{A.8})$$

$$\theta(r, t) = \frac{2}{t - t_B(r)}. \quad (\text{A.9})$$

Here the function $t_B(r)$ has an arbitrary radial profile, but in order that the shear (and electric Weyl tensor) be small, the *size* of radial fluctuations in $t_B(r)$ must not be too large.

To quantify this, consider a homogeneous background solution

$$\rho^{(0)}(t) = \frac{1}{6\pi G(t - t_B^{(0)})^2}, \quad (\text{A.10})$$

$$\theta^{(0)}(t) = \frac{2}{t - t_B^{(0)}}, \quad (\text{A.11})$$

near the perturbed solution (A.8) and (A.9), where $t_B^{(0)}$ is a constant. Define the energy density perturbation by

$$\Delta\rho(r, t) \equiv \rho(r, t) - \rho^{(0)}(t). \quad (\text{A.12})$$

Then, expanding in powers of $\Delta t_B/t$, where $\Delta t_B(r) \equiv t_B(r) - t_B^{(0)}$, we have

$$\frac{\Delta\rho}{\rho^{(0)}} = 2 \frac{\Delta t_B}{t_0} \frac{t_0}{t} + \mathcal{O}\left(\frac{\Delta t_B}{t}\right)^2, \quad (\text{A.13})$$

with t_0 an arbitrary reference time. Comparing this expression with Eq. (A.1), we see that we have indeed isolated the decaying mode, and its amplitude can be read off of Eq. (A.13) as

$$D_2(r) = 2 \frac{\Delta t_B(r)}{t_0}. \quad (\text{A.14})$$

A similar calculation gives

$$\frac{\Delta\theta}{\theta^{(0)}} = \frac{\Delta t_B}{t_0} \frac{t_0}{t} + \mathcal{O}\left(\frac{\Delta t_B}{t}\right)^2, \quad (\text{A.15})$$

which, with Eq. (A.2), again gives Eq. (A.14). Therefore it is *fluctuations* of the bang time $t_B(r)$ that give the decaying mode, and we can set the decaying mode to zero by setting $t_B(r) = \text{const}$.

It is very important to point out that the comparison between the ordinary FRW perturbations $\delta\rho$ and $\delta\theta$ and the perturbations $\Delta\rho$ and $\Delta\theta$ is valid, since the FRW perturbations were specified in comoving gauge, and the LTB solutions Eq. (A.8) and (A.9) are specified with respect to the comoving congruence.

Finally, note that at times early enough that $t \simeq \Delta t_B(r)$, the linear approximation breaks down. This is expected, since the decaying mode diverges at early times. This result is intuitively clear, as we expect differences in ‘‘bang time’’ to become all-important at early times, but to be inconsequential at sufficiently late times.

3. Vanishing decaying mode

Now that we have isolated the LTB decaying mode, we can examine the growing mode, by looking at solutions

with $t_B(r) = 0$, but with nonvanishing curvature of the comoving slices. For definiteness I will consider the open case, ${}^{(3)}R < 0$; the other cases follow similarly.

In this case, Eqs. (A.5) to (A.7) have the solution

$$\rho(r, t) = \rho_0(r) \left(\frac{a_0}{a} \right)^3, \quad (\text{A.16})$$

$$\theta(r, t) = 3 \frac{\dot{a}}{a}, \quad (\text{A.17})$$

where the quantity $a = a(r, t)$ is given parametrically by

$$\frac{a}{a_0} = \frac{1 - \Omega_{K,0}}{2\Omega_{K,0}} (\cosh \eta - 1), \quad (\text{A.18a})$$

$$\theta_0(r)t = \frac{3}{2} \frac{1 - \Omega_{K,0}}{\Omega_{K,0}^{3/2}} (\sinh \eta - \eta). \quad (\text{A.18b})$$

Quantities with subscript 0 are evaluated at reference time $t = t_0$, and are related by

$$(1 - \Omega_{K,0})\theta_0^2 = 24\pi G\rho_0, \quad (\text{A.19})$$

and, by analogy with the homogeneous FRW case, I define

$$\Omega_{K,0}(r) \equiv -\frac{3}{2} \frac{{}^{(3)}R_0}{\theta_0^2}. \quad (\text{A.20})$$

Therefore the solution is determined by one free radial function, which describes the spatial Ricci curvature on some reference comoving slice.

Again, consider a spatially flat homogeneous background solution

$$\rho^{(0)}(t) = \frac{1}{6\pi Gt^2}, \quad (\text{A.21})$$

and define the density perturbation $\Delta\rho$ by Eq. (A.12). If we are to evaluate this perturbation at time t_0 , then for the linear approximation to be valid we require $\Omega_{K,0}(r) \ll 1$, i.e. the perturbation must correspond to a small curvature fluctuation. Then Eq. (A.18b) tells us that $\eta \ll 1$ (this is equivalent to the ‘‘small u ’’ approximation in [39]). We can now solve the set Eq. (A.18) for a/a_0 perturbatively in η . Keeping the next-to-leading order terms in the expansions for the hyperbolic functions, I find

$$\frac{a}{a_0} = (6\pi G\rho_0 t^2)^{1/3} + \frac{1}{80} \frac{1 - \Omega_{K,0}}{\Omega_{K,0}} \eta^4 + \mathcal{O}(\eta^6). \quad (\text{A.22})$$

Combining this with the lowest-order expression

$$\theta_0 t = \frac{1 - \Omega_{K,0}}{4\Omega_{K,0}^{3/2}} \eta^3 + \mathcal{O}(\eta^5) \quad (\text{A.23})$$

gives

$$\frac{a}{a_0} = (6\pi G\rho_0 t^2)^{1/3} \left[1 + \frac{1}{5} \frac{\Omega_{K,0}}{(1 - \Omega_{K,0})^{2/3}} \left(\frac{t}{t_0} \right)^{2/3} \right]. \quad (\text{A.24})$$

Combining this expression with Eq. (A.16) gives

$$\rho(r, t) = \frac{1}{6\pi Gt^2} \left[1 - \frac{3}{5} \frac{\Omega_{K,0}}{(1 - \Omega_{K,0})^{2/3}} \left(\frac{t}{t_0} \right)^{2/3} \right]. \quad (\text{A.25})$$

Therefore the density perturbation is finally determined to be

$$\frac{\Delta\rho}{\rho^{(0)}} = -\frac{3}{5} \Omega_{K,0} \left(\frac{t}{t_0} \right)^{2/3} \quad (\text{A.26})$$

at lowest order. Comparing with Eq. (A.1), we see that, as expected, Eq. (A.26) consists of a pure growing mode. As with the decaying mode case, we can read off the growing mode amplitude as

$$D_1(r) = -\frac{3}{5} \Omega_{K,0}. \quad (\text{A.27})$$

With Eq. (A.20), we recover Eq. (A.3), i.e. the growing mode is given by the spatial curvature, as expected.

A similar calculation gives

$$\frac{\Delta\theta}{\theta^{(0)}} = \frac{1}{5} \Omega_{K,0} \left(\frac{t}{t_0} \right)^{2/3}, \quad (\text{A.28})$$

which, with Eq. (A.27), is again consistent with the FRW expression for the growing expansion perturbation mode, Eq. (A.2). Therefore, the growing mode for LTB spacetimes near FRW is indeed given by the spatial curvature of the comoving slices.

[1] D. W. Hogg et al., *Astrophys. J.* **624**, 54 (2005), arXiv:astro-ph/0411197.
 [2] O. Lahav, *Class. Quant. Grav.* **19**, 3517 (2002),

arXiv:astro-ph/0112524.
 [3] J. Goodman, *Phys. Rev.* **D52**, 1821 (1995), arXiv:astro-ph/9506068.

- [4] R. R. Caldwell and A. Stebbins (2007), arXiv:0711.3459 [astro-ph].
- [5] C. Clarkson, B. A. Bassett, and T. H.-C. Lu (2007), arXiv:0712.3457 [astro-ph].
- [6] J.-P. Uzan, C. Clarkson, and G. F. R. Ellis, Phys. Rev. Lett. **100**, 191303 (2008), arXiv:0801.0068 [astro-ph].
- [7] M.-N. Celerier, Astron. Astrophys. **353**, 63 (2000), arXiv:astro-ph/9907206.
- [8] G. Lemaître, Annales de la Societe Scientifique de Bruxelles **53**, 51 (1933).
- [9] R. C. Tolman, Proc. Nat. Acad. Sci. **20**, 169 (1934).
- [10] H. Bondi, Mon. Not. Roy. Astron. Soc. **107**, 410 (1947).
- [11] H. Alnes, M. Amarzguioui, and O. Gron, Phys. Rev. **D73**, 083519 (2006), arXiv:astro-ph/0512006.
- [12] K. Enqvist and T. Mattsson, JCAP **0702**, 019 (2007), arXiv:astro-ph/0609120.
- [13] S. Alexander, T. Biswas, A. Notari, and D. Vaid (2007), arXiv:0712.0370 [astro-ph].
- [14] J. Garcia-Bellido and T. Haugboelle, JCAP **0804**, 003 (2008), arXiv:0802.1523 [astro-ph].
- [15] K. Enqvist, Gen. Rel. Grav. **40**, 451 (2008), arXiv:0709.2044 [astro-ph].
- [16] P. J. Greenberg, J. Math. Anal. Appl. **30**, 128 (1970).
- [17] C. A. Clarkson and R. K. Barrett, Class. Quant. Grav. **20**, 3855 (2003), arXiv:gr-qc/0209051.
- [18] C. Clarkson, Phys. Rev. **D76**, 104034 (2007), arXiv:0708.1398 [gr-qc].
- [19] C. G. Tsagas, A. Challinor, and R. Maartens, Phys. Rept. (to be published) (2008), arXiv:0705.4397 [astro-ph].
- [20] A. D. Linde, D. A. Linde, and A. Mezhlumian, Phys. Lett. **B345**, 203 (1995), arXiv:hep-th/9411111.
- [21] J. P. Zibin and A. Moss (2008), in preparation.
- [22] R. M. Wald, *General Relativity* (University of Chicago Press, Chicago, 1984).
- [23] H. van Elst and G. F. R. Ellis, Class. Quant. Grav. **13**, 1099 (1996), arXiv:gr-qc/9510044.
- [24] R. A. Sussman and L. Garcia Trujillo, Class. Quant. Grav. **19**, 2897 (2002), arXiv:gr-qc/0105081.
- [25] C. Carbone, C. Baccigalupi, and S. Matarrese, Phys. Rev. **D73**, 063503 (2006), arXiv:astro-ph/0509680.
- [26] H. Mutoh, T. Hirai, and K.-i. Maeda, Phys. Rev. **D55**, 3276 (1997), arXiv:astro-ph/9608183.
- [27] S. Matarrese, O. Pantano, and D. Saez, Phys. Rev. **D47**, 1311 (1993).
- [28] H. van Elst, C. Ugglia, W. M. Lesame, G. F. R. Ellis, and R. Maartens, Class. Quant. Grav. **14**, 1151 (1997), arXiv:gr-qc/9611002.
- [29] J. M. Bardeen, in *Cosmology and Particle Physics*, edited by L.-Z. Fang and A. Zee (Gordon and Breach, New York, 1988), pp. 1–64.
- [30] J.-c. Hwang, Astrophys. J. **375**, 443 (1991).
- [31] E. Komatsu et al. (WMAP) (2008), arXiv:0803.0547 [astro-ph].
- [32] L. Amendola and F. Finelli, Phys. Rev. Lett. **94**, 221303 (2005), arXiv:astro-ph/0411273.
- [33] A. R. Liddle and D. H. Lyth, *Cosmological Inflation and Large-Scale Structure* (Cambridge University Press, Cambridge, 2000).
- [34] J. P. Zibin, A. Moss, and D. Scott, Phys. Rev. **D76**, 123010 (2007), arXiv:0706.4482 [astro-ph].
- [35] S. Ho, C. M. Hirata, N. Padmanabhan, U. Seljak, and N. Bahcall (2008), arXiv:0801.0642 [astro-ph].
- [36] V. F. Mukhanov, H. A. Feldman, and R. H. Brandenberger, Phys. Rept. **215**, 203 (1992).
- [37] J. Silk, Astron. Astrophys. **59**, 53 (1977).
- [38] C. Hellaby and A. Krasinski, Phys. Rev. **D73**, 023518 (2006), arXiv:gr-qc/0510093.
- [39] T. Biswas and A. Notari (2007), arXiv:astro-ph/0702555.
- [40] Note that LTB spacetimes are generically time-dependent, so it is not possible to resolve perturbations into *temporal* harmonics as can be done on the Schwarzschild background, e.g.
- [41] Technically, we expect the tensors to split into even and odd parity modes. Only the even parity tensor modes couple to the scalar modes [18].
- [42] Precisely, the perturbation $\delta\theta$ is defined as the perturbation in the expansion of the comoving worldlines, evaluated on the comoving-orthogonal slices.